University of California

Ernest O. Lawrence
Radiation Laboratory

A FAST, W[illegible] RANGE TIME-TO-HEIGHT CONVERSION SYSTEM

Berkeley, California

DISCLAIMER

UCRL-10425

UNIVERSITY OF CALIFORNIA

Lawrence Radiation Laboratory
Berkeley, California

Contract No. W-7405-eng-48

A FAST, WIDE-RANGE TIME-TO-HEIGHT CONVERSION SYSTEM

Donald L. Wieber

September 18, 1962

A FAST, WIDE-RANGE TIME-TO-HEIGHT CONVERSION SYSTEM

Donald L. Wieber

Lawrence Radiation Laboratory
University of California
Berkeley, California

September 18, 1962

ABSTRACT

A time-to-height conversion system has been developed which is useful for measuring time intervals from 10 ps to 200 μs. When driven by a mercury-relay pulse generator through appropriate fixed delays, the resolution of the system, FWHM, is 6 ps, the apparent time shift with temperature is less than 2 ps/°C, and the integral linearity is within ± 1%. The apparent time distribution through a type 58 AVP photomultiplier tube driven by a mercury-relay light pulser was less than 0.3 ns at a fixed light level equivalent to 10^3 photoelectrons per pulse. The apparent time shift was less than 0.5 ns for variations from 10^2 to 10^4 photoelectrons per pulse.

A FAST, WIDE-RANGE TIME-TO-HEIGHT CONVERSION SYSTEM

Donald L. Wieber

Lawrence Radiation Laboratory
University of California
Berkeley, California

September 18, 1962

1. Introduction

Nuclear particles can often be identified and their energy distributions analyzed by use of time-of-flight techniques[1, 2]. Time-of-flight instrumentation is usually the limiting factor in the resolution and reproducibility of the timing measurements. This equipment must make a precise, accurate decision as to when a nuclear event occurs and translate that decision with maximum fidelity and stability into a meaningful record.

This report describes a time-to-height conversion system, which is presently being used at this Laboratory (see Fig. 1). The system is useful for measuring time intervals from 10 ps to 200 μs. Driven by mercury-relay-formed fast-rising test pulses through appropriate fixed delays, with the setup of Fig. 2, the full width at half-maximum amplitude (FWHM) on the pulse-height analyzer is two channels (6 ps). The apparent time shift with temperature is less than 2 ps/°C. The integral linearity is ± 1%, as shown in Fig. 3. In a test using a type-58AVP photomultiplier tube, the apparent time shift was less than 0.5 ns for a variation in light level equivalent to from 10^2 to 10^4 photoelectrons per pulse. The FWHM at a fixed level of 10^3 photoelectrons per pulse was less than 0.3 ns.

Signals used to indicate the time of occurence of a nuclear event vary in amplitude. A decision, not influenced by signal amplitude, must be made as to the arrival time of the signal, and this information presented as a standardized, fast-rising pulse. The triggering level and the circuit delay must be as stable as possible.

For a pulse of fixed shape and size whose leading edge is related through a constant delay to the time of interest, a coincidence circuit or a time-to-height converter may be used to measure that time with respect to some reference time. Usually, many such events are recorded and eventually presented as a time-distribution histogram.

In the coincidence method, one may use a single coincidence circuit[1, 2, 3] with a variable reference input delay, or there may be many parallel coincidence circuits[4, 5], distributed at varied or equal time increments, which sort and route the signals with respect to their arrival time. Recently, tunnel-diode coincidence circuits have been developed at this laboratory which have coincidence curve widths of 150 ps with edges as steep as 10 ps/c per decade.[3] Although the coincidence method is more straightforward and promises the best ultimate system resolution and repetition rate, acquisition of a time-distribution histrogram with a single coincidence circuit is tedious. The multi-coincidence or "chronotron" system overcomes this disadvantage, but its usefulness is limited by system complexity and its ultimate resolution is limited, to first order, by the coincidence curve width. The information out of a chronotron is of such form as to be best fed directly into a memory unit. This requires either a special memory system or the modification of a pulse-height analyzer to provide direct access to its memory.

Therefore, work continues on the development of time-to-height conversion systems[6, 7]. Such a system translates the time information into a pulse height which is readily analyzed by conventional pulse-height analyzers. Time-to-height conversion is essentially a simple process involving a minimum of circuit complexity. To convert a time interval to a related pulse height, the shaped timing pulses are used to switch a constant current, I, into a fixed capacitor, C, during the time interval, τ, to be measured. In such a circuit

the voltage across the capacitor, V_c, is a linear function of the time interval, $V_c = I/C\,\tau$, where I/C is constant. The converted output is not quantized and therefore more susceptible to noise than the coincidence systems. In general, more switching energy is required for present time-to-height converters than for a tunnel-diode coincidence circuit[3]. This energy is usually gained at the expense of bandwidth and stability. The output of the time-to-height converter should be of the size and shape required by a pulse-height analyzer. At present, this is roughly 1 μs in width and a few V in amplitude.

In general a time-to-height conversion system requires:

a. a pulse-shaping circuit that indicates the time of arrival of a particle and presents this information, with maximum fidelity, as a standardized, fast rising pulse,

b. an analogue time-to-height converter that presents a shaped output whose amplitude is a linear, stable function of the time interval between the leading edges of two shaped input pulses,

c. minimum noise and maximum stability in all elements.

2. Discriminator-Shapers

Scintillation counters mounted on photomultiplier tubes remain the most popular and successful means of detecting nuclear events for time-of-flight analysis. The photomultiplier tube has gain-bandwidth and signal-to-noise figures which are as yet unattainable by other conventional means. Most fast timing work at this laboratory has been done with photomultipliers, and it is this work to which we will refer. In particular, Bjerke et al. have developed "zero-crossing" timing techniques which, when used with discriminators and coincidence circuits using high-current tunnel diodes, give timing resolutions that are to first order limited only by photomultiplier time spread[3, 8]. Time spreads calculated from this data are shown in Table I with corresponding data measured independently with out time-to-height conversion system. The experiments show substantial agreement.

As shown by Bjerke et al, zero-crossing techniques provide a way of using most of the timing information in a phototube pulse by inspecting most of the pulse, thereby minimizing time-shift as a function of pulse height[8]. The photomultiplier signal, Fig. 4a, is "differentiated" to cause the signal to cross back over zero as in Fig. 4b. A discriminator is set to trigger just after the zero-crossing point, above the noise level. This method is most effective if the discriminator triggers quickly on very little differential charge. A 5-mA tunnel diode can be stably biased to within 0.5 mA of its peak current and can be switched in about 1 ns[9]. This implies a required trigger charge of only 5 pC.

Because the negative conductance increases almost as a direct function of peak current, and since higher switching currents charge stray capacitances more quickly, best short-term timing results can be obtained by using high-current tunnel diodes[3]. However, the nominal peak-current drift with temperature is also a direct function of peak current. That is, a 50-mA tunnel diode might be expected to show 50 times more peak current drift with temperature than would a 1-mA type[9]. Because the threshold of our tunnel-diode discriminators is determined by the difference between the tunnel-diode peak current and an adjustable bias current, peak current drift with temperature shows up directly as a shift in threshold. The tunnel diode selected for the time-to-height converters was a compromise, having a nominal peak current of 5 mA.

The charge sensitivity of the discriminator is reflected directly in the curve of Fig. 5. The shape of this curve is common to all simple regenerative circuits and is of the general form of the curve, $XY = K$, intersecting a straight line, $Y = K'$, where K' is the nominal minimum circuit delay. This curve shows that, as the input voltage is decreased toward the threshold value, a longer time is required to accumulate the necessary trigger charge. From this, it is

apparent that the high charge sensitivity of the tunnel diode minimizes time shift at low input signal levels.

The time-to-height converter start and stop discriminators are identical. The start and stop shapers are nearly complements of each other. In the following discussion, we will refer to the "start" discriminator-shaper, Figs. 6 and 7. Transistor Q_1 is introduced, at the expense of discriminator speed, to allow a matched input impedance of 125Ω. The common-base configuration was chosen for maximum bandwidth, minimum reflection at the input due to tunnel-diode switching, and maximum driving impedance for the tunnel diode. The common-base input stage is also conveniently adapted to the use of the delay-shift compensating capacitor, C_x (FIG. 10). This capacitor shifts the zero-crossing time, which tends to compensate for the normal discriminator delay shift near theresold, as shown in Fig. 8. An example of a first-order calculation of C_x is given in the Appendix. Capacitor C_x is useful when timing information must be derived from zero-crossing signals with amplitudes near threshold. This is in preference to amplification of the photomultiplier signal, which destorts pulse shapes and introduces further timing errors for large signal variations. Although the use of C_x will be helpful in some cases, it is only a means of compensation for, not elimination of, delay shift with amplitude.

Diodes CR_1, CR_2, and CR_3 with transistor Q_2, form a gate which, with switch S_1 closed, raises the discriminator threshold to 5 V. A positive 2- to 4-V gate signal opens the gate. With S_1 open, the gate is normally open.

The tunnel diode, CR_4, is biased and loaded so that it operates in a monostable manner. The forward bias current is determined by the setting of R_{14}. With a discriminator input impedance of 125Ω, the threshold as referred to the input can be varied from 10 to 600 mV. The threshold is nearly constant for repetition rates up to 10 Mc at maximum sensitivity and 5 Mc at minimum sensitivity. The input pulse width should be kept below 100 ns to avoid double pulsing.

Transistors Q_4 and Q_5 form a complementary, emitter-coupled, one-shot multivibrator. Both transistors are biased in their acitve regions. The feedback loop is held open by CR_6 which is normally nonconducting. The tunnel-diode signal appearing at the base of Q_4 lowers the impedance of CR_6, causing the circuit to regenerate. Since both transistors are in their active regions during trigger and pulse rise, the trigger delay is less than 1 ns. The rise time at the emitter of Q_6 is about 3 ns; the pulse height is about 5 V. Maximum duty cycle is about 40%. The temperature dependence of dc transistor parameters causes the one-shot trigger threshold to be slightly temperature-dependent. Because of the sharp leading edge of the trigger, the threshold variation results in a trigger delay shift of less than 5 ps/°C. The time shift in the stop channel tends to be the same, reducing the composite effect at the converter.

By selection of C_{17}, the one-shot pulse width can be varied from 0.5 μs to over 1 ms with negligible deterioration of pulse shape. The required pulse width is determined by the sum of the maximum time interval to be measured and the minimum pulse width required by the pulse-height analyzer. During the pulse, Q_5 is saturated much harder than Q_4. The pulse will not end until Q_5 turns off. Therefore, the time required to pull Q_5 out of saturation will effect the total output pulse width. Q_5 is a 2N834 which has a turn-off time in this circuit of less than 50 ns. The equivalent transistor Q_5 in the stop circuit is a 2N1143 (Figs. 9 and 10). The turn-off time of an epitaxial 2N1143 in this circuit is about 100 ns. A non epitaxial 2N1143 may require as long as 500 μs. Consequently, with equal values of the feedback capacitor, C_7(of Figs. 9 and 10) = C_{17} (of Figs. 6 and 7), the stop pulse will always be longer than the start pulse. This is a requirement of the analogue conversion circuit.

3. Time-To-Height Converter

The time, τ, between the leading edge of the start pulse and the leading edge of the stop pulse is converted into a related pulse height by means of a constant current, I, charging a capacitor, C_2, for the time, τ. Referring to Fig. 11, transistors Q_1 and Q_2, with diodes CR_4, CR_5, and CR_6, form a wide-bandwidth constant-current source. Diodes CR_5 and CR_6 serve to compensate for the temperature drift of the Q_1 and Q_2 emitter-base junctions. The current I through R_3 varies less than $0.02\%/^{\circ}C$. To maximize the signal-to-noise ratio, I/C should be as large as possible. The minimum value of C_2 is usually fixed at some value much larger than parallel stray capacities, typically 100 pF[7]. Some compromise must be reached between maximizing I and concern for the high-current high-frequency characteristics of the current switches. The current-switching elements were chosen on the basis of quickest recovery time and least change in the charge in analogue capacitor C_2 due to stored charge in the switches and direct feedthrough from the driving signals. Either a saturated transistor or a forward-conducting diode stores some quantity of minority carriers which must be swept out or recombined before the device can be switched off. In each case the amount of stored charge is a significant function of the driving signal and temperature. This has been the limiting factor in the stability of some previous solid-state circuits[7]. A Hughes diode, HD5000, was found to recover in less than 1 ns in our time-to-height converter circuit. The change in charge at C_2 due to diffusion and depletion capacities was nearly negligible. This, in addition to attendant circuit simplicity, led to the choice of HD5000 diodes as converter current-switching elements.

These diodes, CR_2 and CR_3, conduct the constant current I at quiescence. They are arranged in the circuit so than any feedthrough from one tends to be compensated at C_2 by feedthrough from the other. The arrival of a negative start pulse at the anode of CR_2 causes it to become nonconducting, forcing the current I to charge C_2. The voltage across C_2 then rises linearly at a rate determined by I/C_2 until either CR_2 or CR_1 begins to conduct. In the absence of a stop pulse, the maximum voltage to which C_2 can rise is limited by the negative bias voltage at the anode of CR_1 or the negative signal voltage at the anode of CR_2. Therefore the maximum linear range is limited by the smaller of these two inverse diode voltages and the capacitor voltage rate of $\Delta V_c/\Delta T = I/C_2$. The maximum time interval that can be converted is $\tau_{max} = V_{c\ max} C_c/I$. For integral linearity of within ± 1%, τ_{max} (μs) ≥ 300 C_2 (μF).

Arrival of a positive stop voltage at the anode of CR_1 causes that diode to conduct, shunting the current I around C_2 and causing CR_3 to become nonconducting.

While both start and stop pulses remain, C_2 can discharge only into the input impedance of the White emitter follower, which is approximately 42 kΩ. As previously pointed out, the start pulse ends before the stop pulse ends. The end of the start pulse allows CR_2 to conduct, discharging C_2 through the low impedance of the start-circuit output emitter follower. The end of the stop pulse leaves the circuit in its quiescent condition. The pulse width out of the converter is then controlled by the width of the start pulse. Since the output is usually fed to a pulse-height analyzer, the pulse width for fast time-of-flight analysis is usually fixed at about 1 μs. Note that in any case the start and stop pulse widths must be at least as long as the time interval to be measured. The duty cycle of the system to this point is limited only by the maximum duty cycle of the driving circuits, which is approximately 40%. For our experiments, the repetition rate has been limited to about 50kc by the pulse-height analyzer.

For large values of C_2, the rise time of the converter output may well be slow enough to confuse the pulse-height analyzer. For these time ranges, Q_6 and the circuit included within the dashed box of Fig. 11 may be added. Q_6 is normally saturated, shunting the output signal to ground. The stop pulse is applied to the base of Q_6, cutting Q_6 off. This allows the output voltage to rise to that of capacitor C_2 in less than 0.1 μs. The pedestal at the converter output caused by this gated operation is less than 50 mV (2% of maximum signal).

The configuration of the White emitter follower was chosen after unsuccessful investigations of complementary and other feedback-type emitter followers. In general, design of fast, feedback-type emitter followers is complicated by their tendency to present a loop gain of greater than unity at some frequencies, causing oscillation and unstable gain. This problem is the result of phase shift in the feedback loop and is generally avoided by slowing the response of the circuit. A loop gain of greater than unity tends to turn one of the base-emitter diodes off, especially in the case of a capacitive load. This leads to further instability and some nonlinearity. In the circuit of Fig. 11, the negative going signal presented to the base of Q_3 tends to reduce its current. However, the amplified signal at the base Q_4 tends to turn Q_4 on, and the feedback signal arriving at the emitter of Q_3 tends to drive that transistor, too, further into conduction. Therefore, if the loop gain tends to become greater than unity, both transistors are driven into higher conduction and the output voltage is referred even more closely to the input.

4. Amplifier-Output Stages

The maximum output voltage of the converter is about 2.5 V. Most solid-state pulse-height analyzers require 6 to 8 V full scale. Also, it is convenient to be able to vary the overall conversion ratio without changing the fast converter circuitry. Therefore, a linear, variable-gain amplifier is useful, although not always necessary, between the converter and the pulse-height analyzer. For

the tests included in this report, amplifier stages shown in Figs. 12 and 13 were used. They are described briefly in the Appendix.

5. Test and Results

The test setup shown in Fig. 2 was used to determine noise, stability, and linearity of the time-to-height conversion system, including the linear amplifiers. A mercury pulser provides two simultaneous outputs with rise times of less than 1 ns. These were fed through appropriate delays to the start and stop discriminator-shapers. The analogue capacitor C_2 of Fig. 11, was set at 150 pF. Conversion gain at the output of the converter, $\Delta V_c/\tau \simeq I/C_2 = 67$ mV/ns.

The resolution over 1-h period at room temperature was two channels (6ps) FWHM with $\tau_{max} = 300\ C_2 = 45$ ns. The resolution may be expressed as the ratio $\tau_{max}/\Delta\tau = (45\times10^{-9})/(6\times10^{-12}) = 7500$ to 1. About 90% of this spread is due to trigger jitter; about 10% is introduced after the converter. Therefore, at high values of C_2, $\tau_{max}/\Delta\tau$ was observed to increase almost in direct proportion to C_2 until the resolution was less than one channel.

The apparent time shift with temperature is less than 2 ps/°C from 20 to 55°C and is a negligible function of C_2. The integral linearity is ±1% to 50 ns as shown in Fig. 3. For higher values of C_2 the linearity remains ±1% to τ_{max}, there τ max (μs) = 300 C_2(μF).

The time resolution of the time-to-height conversion system with a type-58AVP photomultiplier was studied by using the setup shown in Fig. 14. The mercury light pulses [10] was adjusted to provide a known number of photoelectrons per pulse from the photocathode of the 58AVP and a synchronized electrical pulse for use as a start signal for the time-to-height converter. Table I shows the timing resolution, FWHM, and the peak-time shift as a function of light level and photomultiplier gain. The absolute delay through the tube is given parenthetically in the 5000 photoelectron-level row of Table I for each gain setting.

Time spread of the photomultiplier as a function of light level follows Poisson statistics[3]. To first order, for the light levels considered here the photomultiplier time spread will decrease as the square root of the light level. Study of the time spread of type-58AVP photomultipliers preformed previously by Bjerke et al[3], using fast tunnel-diode coincidence techniques, indicated resolutions as given in the last column of Table I. The descrepancy in results for light levels of greater than 100 equivalent photoelectrons per pulse can be attributed to differences in individual tubes, and possible errors in determining the absolute light level. Below 100 photoelectrons per pulse the sensitivity of the time-to-height converter discriminator begins to impair the resolution. This is verified by the shift in peak time at these light levels. The average delay in the photomultiplier should not be a function of the light level. At high light levels some apparent time shift with light level may occur because of tube-gain nonlinearities. At low light levels, however, this should be negligible, and any shift in delay with light level suggests signal levels near the threshold of the discriminator. As the discriminator input voltages approach threshold, statistical amplitude variations cause depreciation of system resolution. Improvement in system resolution with increase in photomultiplier gain at these low light levels is further corroborative evidence.

Note too, from Table I, the reduction in peak-time shift as a function of light level when C_x (as calculated in the Appendix) is added. Study of the time spread in various photomultipliers is being continued.

6. Conclusion

A solid-state time-to-height converter has been developed which is usable over time ranges from 10 ps to 200 μs. With mercury-relay-formed, fast-rising test pulses applied to the discriminator inputs, the system measures a fixed delay with a resolution of 6 ps, or less than one part in 7500. The

observed drift with temperature is less than 2 ps/°C. Preliminary results of timing experiments with a type-58AVP photomultiplier show time shifts of less than 0.5 ns for light-level variations equivalent to from 100 to 10,000 photoelectrons per pulse.

7. Appendix

7.1 CALCULATION OF COMPENSATING CAPACITOR, C_x

As noted in the text, the action of C_x is to cause a shift in zero-crossing time which tends to compensate for the normal discriminator delay shift near threshold, as shown in Fig. 8. The data for Fig. 8 are calculated using the peak-time shift as a function of light level.

The optimum value for C_x is a function of input pulse shape; however, by using several crude approximations, a nominal value may be calculated. For example, note that most of the delay shift shown in Fig. 8a occurs when V_+ is near 0.5 V. Referring to the circuit of Fig. 10, we bias Q_1 so that it will turn off at +0.5 V input. This requires a standby emitter current, I_E, of

$$I_E = \frac{0.5}{125} = 4 \text{ mA}$$

and

$$R_{36} \simeq \frac{24}{4} = 6\text{k} \simeq 5.6\text{k}.$$

When V_+ remains below 0.5 V, C_x is shunted by the input impedance of Q_1, which is about 5Ω at quiescence. For V_+ greater than 0.5 V, C_x is shunted by a nonconducting diode and the voltage across C_x, V_c, rises with a time constant $\tau_1 = 120\ C_x$. If we assume a τ_1 much shorter than the input pulse width, V_c will reach V_+. Furthermore, we shall assume that the peak negative excursion,

V_-, is one-half V_+. Then if the input voltage were to fall much faster than V_c and since zero voltage is about 66% of the peak-to-peak swing, zero-crossing would be delayed by about the time interval, τ_1. Inspecting Fig. 7a we choose a τ_1 of 1 ns. Then we have $C_x = 10^{-9}/120 \approx 10$ pF. The effect of adding $C_x = 10$ pF can be seen in Fig. 8b and Table I. It should be obvious that the calculations shown above are approximate and only give a nominal value for C_x. The optimum value should be emperically determined for a particular pulse shape, with the nominal value of C_x used as a starting point.

7.2 CHARACTERISTICS OF AMPLIFIER STAGES

A. Variable-Gain Linear Amplifier (Fig. 12)

The amplifier consists of two feedback-pair stages designed for optimum linearity and stability. The gain is controlled by means of feedback resistors from 1 to 4 in increments of 0.5 and from 4 to 16 in increments of 2.

The nominal input impedance of 1k is divided between 511Ω on the amplifier board and 464 Ω on the converter board. An alternate front panel input is provided which has an internal input impedance of 1k. The amplifier accepts positive or negative input, and is designed to drive an impedance of 1k with ±1% integral linearity from 0 to ±4 V.

B. Output Stage

The output stage consists of a feedback-pair stage with a fixed gain of 4 driving a White emitter follower. Components R_3, R_4, and C_5 form an integrating network to improve the signal-to-noise ratio. This stage accepts negative inputs and is also designed to drive a dc impedance of 1kΩ, but will drive very long cables with ±1% integral linearity from 0 to +8 V.

Acknowlegments

We wish to thank the many people whose advice and assistance were instrumental in the design, testing, and reporting of this work. In particular, thanks are due to Mr. C. R. Kerns, who led us brilliantly in our investigations of phototube time distributions, and Mr. D. A. Mack who contributed basic technical advice and particular aid in the preparation of this report.

References

1. D. B. James and P. B. Treacy, Proc. Phys. Soc. (London) A64 (1951) 847.
2. L. E. Beghran, R. A. Allen, J. M. Calvert, and H. Halbon, Phys. Rev. 86 (1952) 1044.
3. A. E. Bjerke, Q. A. Kerns, and T. A. Nunamaker, "Time Resolution of a Scintillation Counter System," Lawrence Radiation Laboratory Report UCRL-9976, February 1962.
4. J. W. Keuffel, Rev. Sci. Instr. 20 (1949) 197.
5. A. E. Bjerke, A. A. Kerns, and T. A. Nunamaker, "A Solid-State Chronotron for Digitizing Time Delays," Lawrence Radiation Laboratory Report UCRL-9270, December 1960.
6. G. C. Neilson and D. B. James, Rev. Sci. Instr. 26 (1955) 1018.
7. C. Culligan and N. H. Lipman, Rev. Sci. Instr. 31 (1960) 1209.
8. A. E. Bjerke, Q. A. Kerns, and T. A. Nunamaker, "Pulse Shaping and Standardizing of Photomultiplier Signal for Optimum Timing Information Using Tunnel Diodes," Lawrence Radiation Laboratory Report UCRL-9838, August 1961.
9. H. R. Lowry, J. Giorgis, E. Gottlieb, and R. C. Weischedel, General Electric Tunnel Diode Manual, 1st edition (General Electric Co. Liverpool, N. Y., 1961)
10. Q. A. Kerns, F. A. Kirsten, and G. C. Cox, Rev. Sci. Instr. 26 (1959) 31.

Table I. Time resolution of 58AVP photomultiplier tube

Light level (photoelectrons per pulse)		Time-to-height converter					Coincidence
	Pm gain =	10^6	2×10^6	5×10^6	10^6	5×10^6	10^6
	C_x(pF)=[a]	10	10	10	0	0	—
5000	Peak[b, c] shift	0 (90.0 ns)	0 (88.5 ns)	0 (86.5 ns)	0 (88.5 ns)	0 (85.1 ns)	—
5000	Resol.[b, d]	0.1	0.15	0.16	0.2	0.2	0.18
2500	Peak shift	0.1	0.1	-0.1	0.3	0.1	—
2500	Resol.	0.17	0.18	0.15	0.2	0.2	0.21
1000	Peak shift	-0.1	0.3	0.1	0.6	0.1	—
1000	Resol.	0.26	0.28	0.29	0.4	0.3	0.32
500	Peak shift	-0.5	0	0.3	0.8	0.5	—
500	Resol.	0.36	0.35	0.43	0.6	0.5	0.37
100	Peak shift	0.3	0	-0.2	1.9	0.9	—
100	Resol.	0.82	0.85	0.81	1.0	0.9	0.67
50	Peak shift	0.7	0.2	-1.5	2.4	1.1	—
50	Resol.	2.1	1.07	1.0	2.1	1.0	0.81

[a] see Fig. 8 and the text.

[b] converted from number of channels to time in nanoseconds

[c] peak shift is the deviation from peak values with the light level at 5000 photoelectrons per pulse

[d] resolution is the full width at half maximum

FIGURE LEGENDS

Fig. 1. Block diagram of time-to-height conversion system.

Fig. 2. Block diagram of the test setup for the time-to-height conversion.

Fig. 3. Linearity of the time-to-height conversion system, C_3 = 150 pF (see Fig. 11).

Fig. 4. Type-58AVP photomultiplier output waveforms. Each division represents 1 ns or 0.3 V. The input light pulses resulted in about 500 photocathode electrons per pulse. The phototube gain was about 10^6. (a) Dynode 14 voltage; (b) anode voltage through differentiating transformer.

Fig. 5. Delay shift of discriminator-shaper as a function of input pulse amplitude for a step input. The threshold voltage is 30 mV; $C_x = 0$.

Fig. 6. Block diagram of the start discriminator-shaper.

Fig. 7. Schematic diagram of the start discriminator-shaper; C_{17} (μF) = τ_{start} (μs)/1470.

Fig. 8. Delay shift of discriminator-shaper as a function of photocathode light level. At low light levels, a pulse of 250 photocathode electrons produces a V_+ of 1 V. (a) C_x = 0 pF; (b) C_x = 10 pF.

Fig. 9. Block diagram of the stop discriminator-shaper.

Fig. 10. Schematic diagram of the stop discriminator-shaper; C_7 (μF) $\approx$ τ_{start} (μs)/1470; $\tau_{stop} \approx \tau_{start}$ + 0.2 μs.

Fig. 11. Schematic diagram of the time-to-height converter.

Fig. 12. Schematic diagram of variable-gain linear amplifier.

Fig. 13. Schematic diagram of linear amplifier output.

Fig. 14. Block diagram of photomultiplier time-distribution experiment.

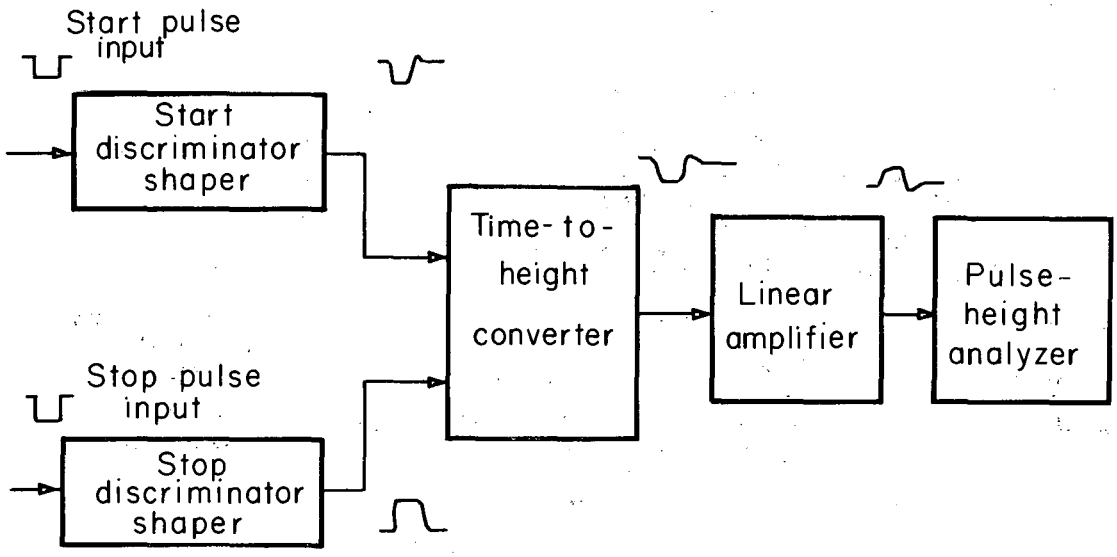
Start pulse input
Start discriminator shaper
Stop pulse input
Stop discriminator shaper
Time-to-height converter
Linear amplifier
Pulse-height analyzer
MU-28790

Fig. 1

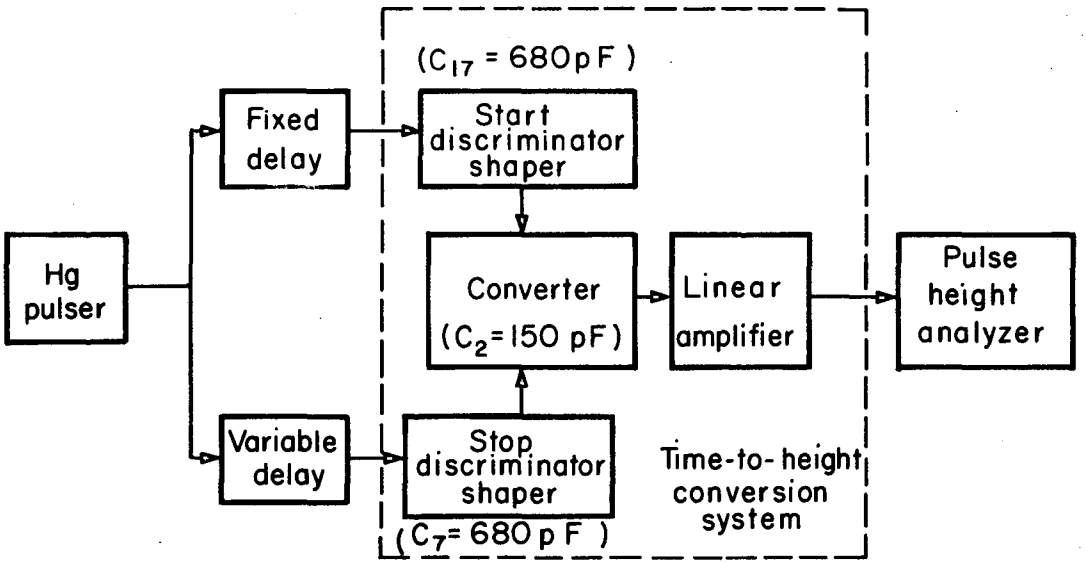
(C_{17} = 680pF)
Fixed delay
Start discriminator shaper
Hg pulser
Converter (C_2=150 pF)
Linear amplifier
Pulse height analyzer
Variable delay
Stop discriminator shaper
(C_7= 680 pF)
Time-to-height conversion system
MU-28791

Fig. 2

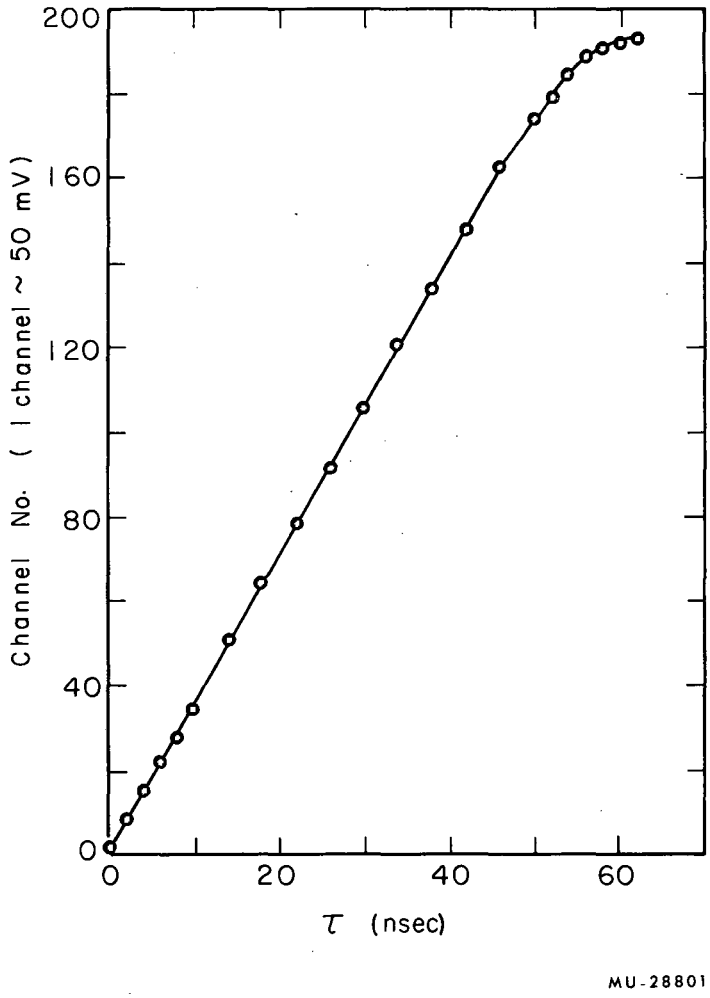
200
160
120
80
40
0
Channel No. (1 channel ~ 50 mV)
0
20
40
60
τ (nsec)
MU-28801

Fig. 3

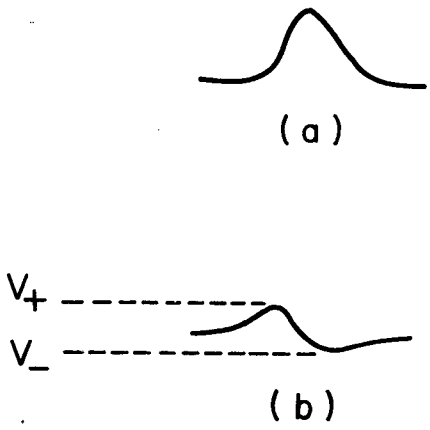

MU-28793

Fig. 4

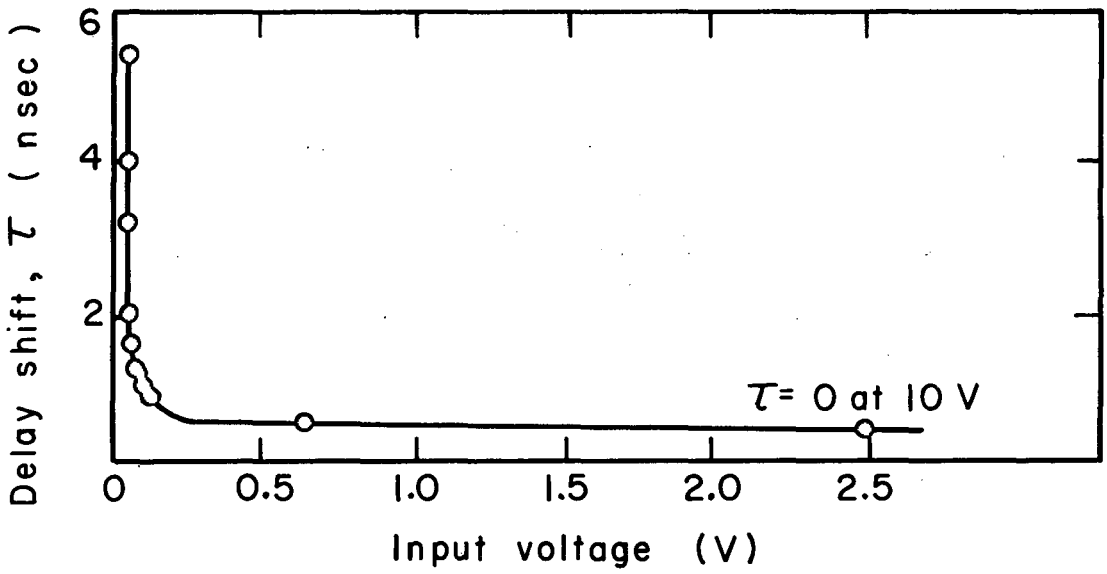

MU-28794

Fig. 5

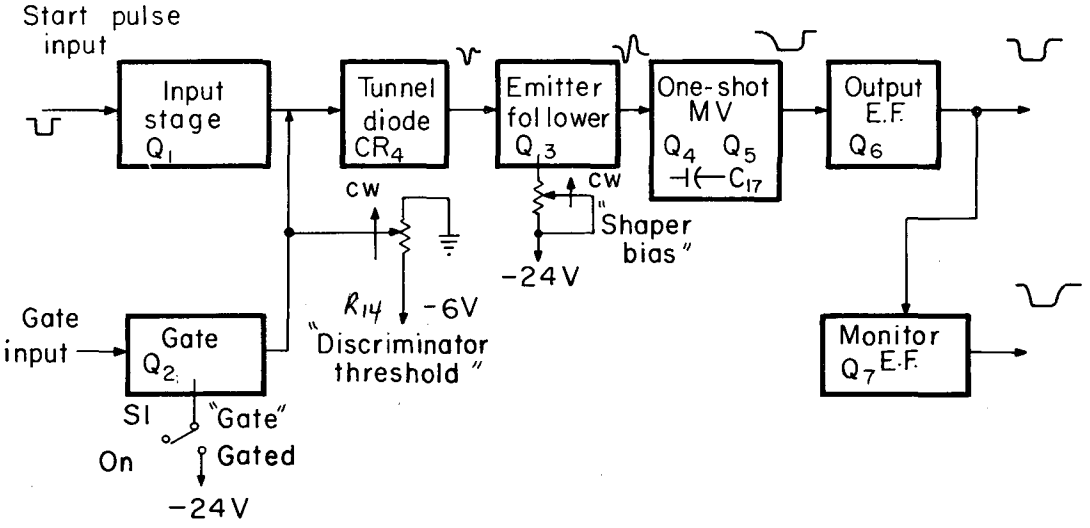
Start pulse input
Input stage Q_1
Tunnel diode CR_4
Emitter follower Q_3
One-shot MV Q_4 Q_5 C_{17}
Output E.F. Q_6
cw
"Shaper bias"
-24V
R_{14}
-6V
"Discriminator threshold"
Gate input
Gate Q_2
SI
"Gate"
On
Gated
-24V
Monitor Q_7 E.F.
MU-28800

Fig. 6

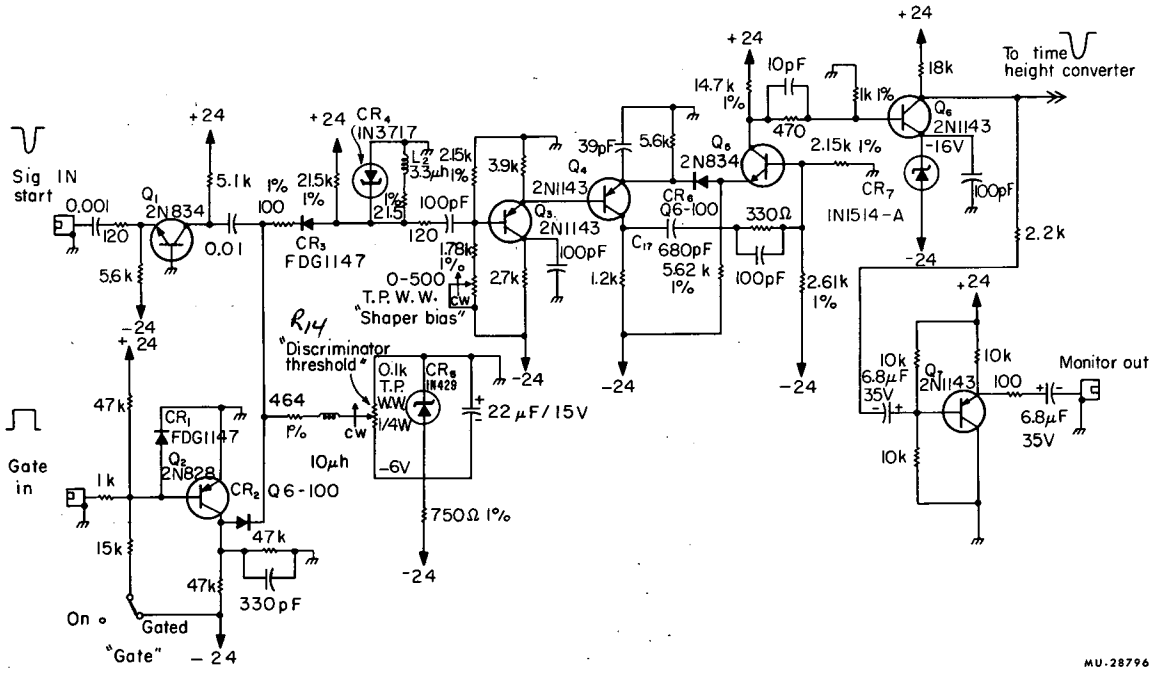
Sig IN start
Gate in
On
Gated
"Gate"
Q1 2N834
Q2 2N828
Q3 2N1143
Q4 2N1143
Q5 2N834
Q6 2N1143
Q7 2N1143
CR1 FDG1147
CR2 Q6-100
CR3 FDG1147
CR4 IN3717
CR5 IN429
CR6 Q6-100
CR7 IN1514-A
R14
"Discriminator threshold"
T.P. W.W. "Shaper bias"
To time height converter
Monitor out
MU-28796

Fig. 7

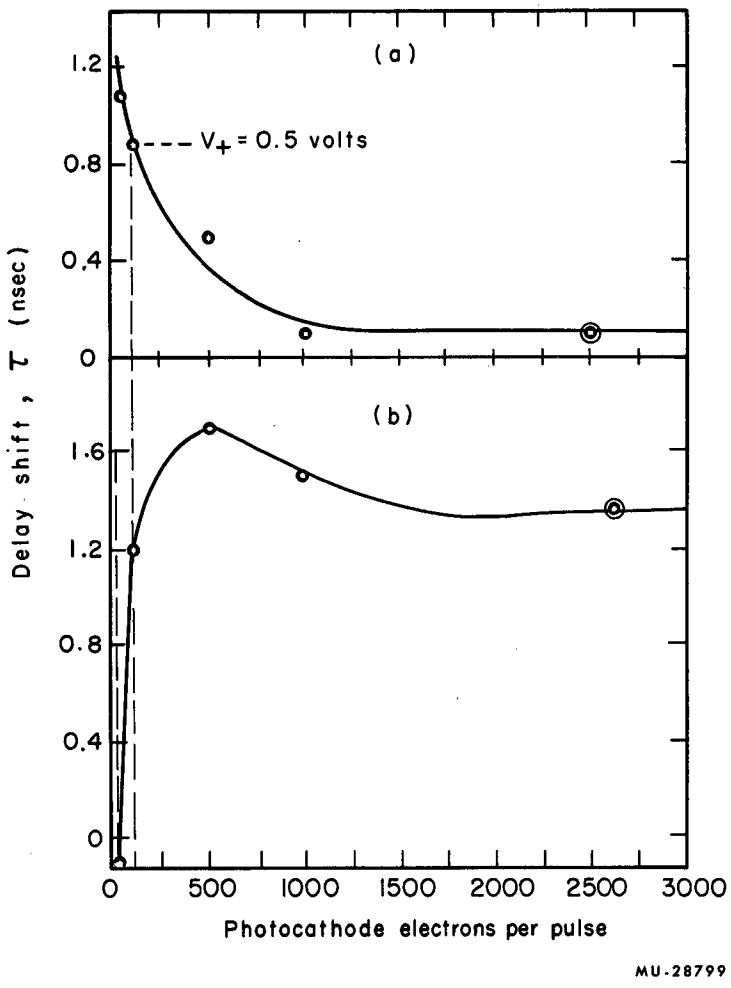
(a)
V_+ = 0.5 volts
(b)
Delay shift, τ (nsec)
1.2
0.8
0.4
0
1.6
1.2
0.8
0.4
0
0
500
1000
1500
2000
2500
3000
Photocathode electrons per pulse
MU-28799

Fig. 8

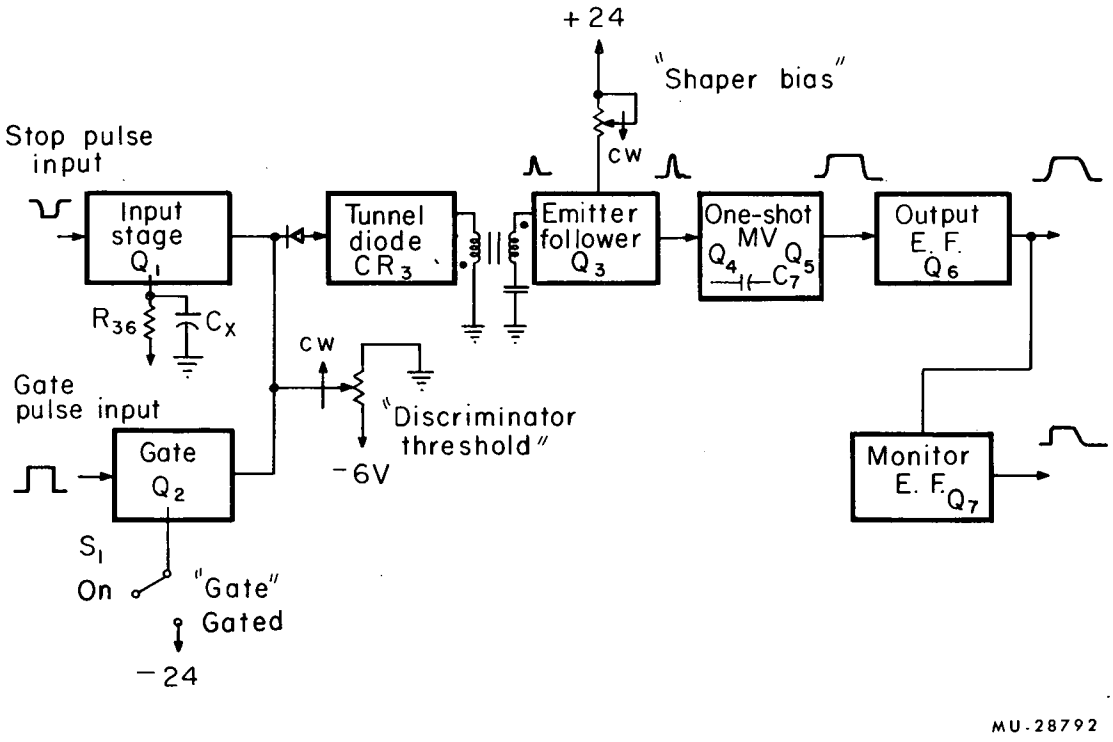
+24
"Shaper bias"
cw
Stop pulse input
Input stage Q_1
Tunnel diode CR_3
Emitter follower Q_3
One-shot MV Q_4 Q_5 C_7
Output E. F. Q_6
R_{36}
C_X
cw
Gate pulse input
"Discriminator threshold"
Gate Q_2
-6V
Monitor E. F. Q_7
S_1
On
"Gate"
Gated
-24
MU-28792

Fig. 9

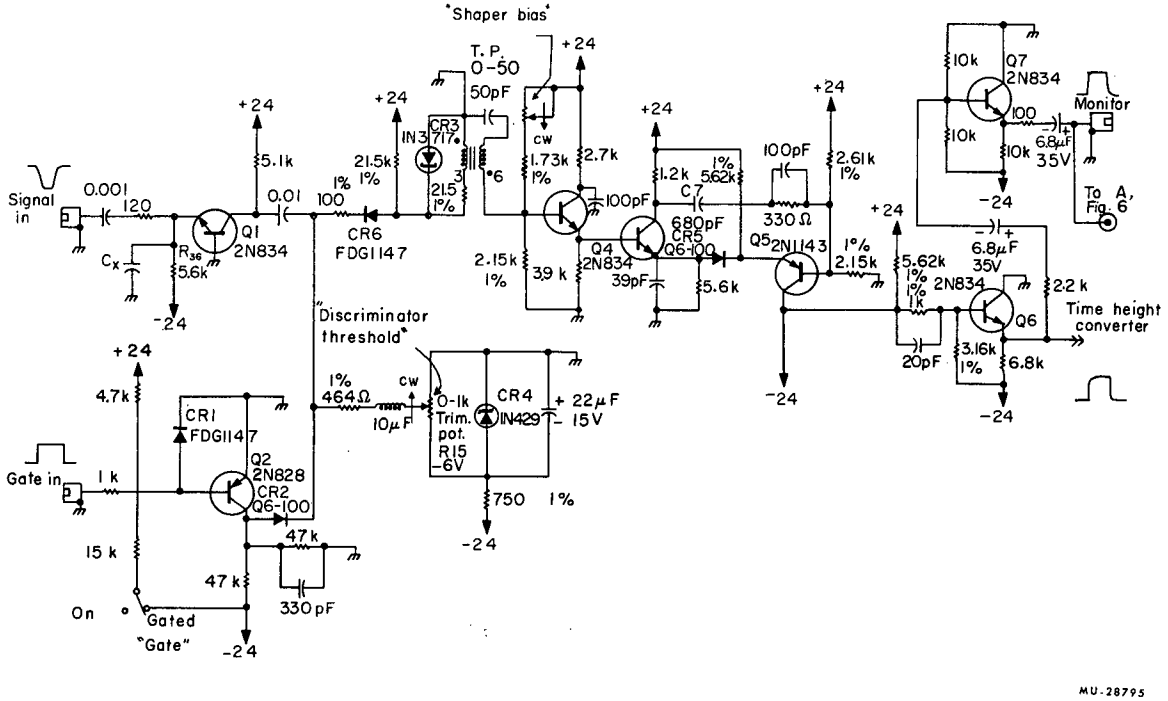
"Shaper bias"
T. P.
0-50
50pF
+24
Signal in
0.001
120
Q1
2N834
C_x
R_{36}
5.6k
-24
5.1k
0.01
100
CR6
FDG1147
21.5k
1%
IN3717
CR3
21.5
1%
cw
1.73k
1%
2.7k
•6
3
100pF
2.15k
1%
3.9 k
Q4
2N834
39pF
1.2k
1%
562k
C7
680pF
CR5
Q6-100
5.6k
100pF
330Ω
Q5 2N1143
1%
2.15k
2.61k
1%
10k
Q7
2N834
100
10k
6.8μF
35V
Monitor
To A, Fig. 6
5.62k
1%
1%
1K
2N834
Q6
2.2 k
Time height converter
20pF
3.16k
1%
6.8k
"Discriminator threshold"
1%
464Ω
cw
10μF
0-1k
Trim. pot.
R15
-6V
CR4
IN429
+ 22μF
- 15V
750 1%
4.7k
CR1
FDG1147
Gate in
1 k
Q2
2N828
CR2
Q6-100
15 k
47 k
47 k
330 pF
On
Gated
"Gate"
MU-28795

Fig. 10

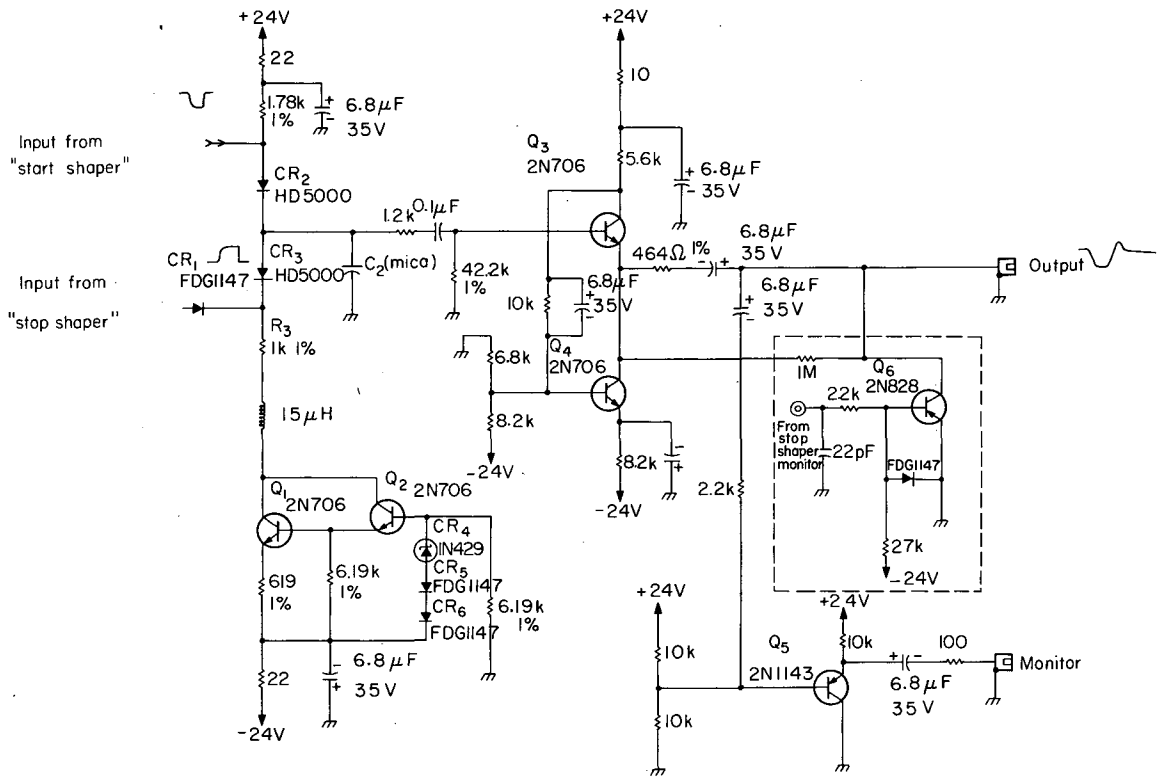
+24V
22
1.78k 1%
6.8μF 35V
Input from "start shaper"
CR2 HD5000
1.2k
0.1μF
CR1 FDG1147
CR3 HD5000
C2(mica)
42.2k 1%
Input from "stop shaper"
R3 1k 1%
15μH
Q1 2N706
Q2 2N706
CR4 IN429
CR5 FDG1147
CR6 FDG1147
619 1%
6.19k 1%
6.19k 1%
22
6.8μF 35V
-24V
+24V
10
Q3 2N706
5.6k
6.8μF 35V
464Ω 1%
6.8μF 35V
10k
6.8μF 35V
6.8μF 35V
Output
Q4 2N706
6.8k
8.2k
-24V
8.2k
2.2k
-24V
IM
Q6 2N828
22k
From stop shaper monitor
22pF
FDG1147
27k
-24V
+24V
+24V
10k
10k
Q5 2N1143
10k
100
6.8μF 35V
Monitor
MUB-1487

Fig. 11

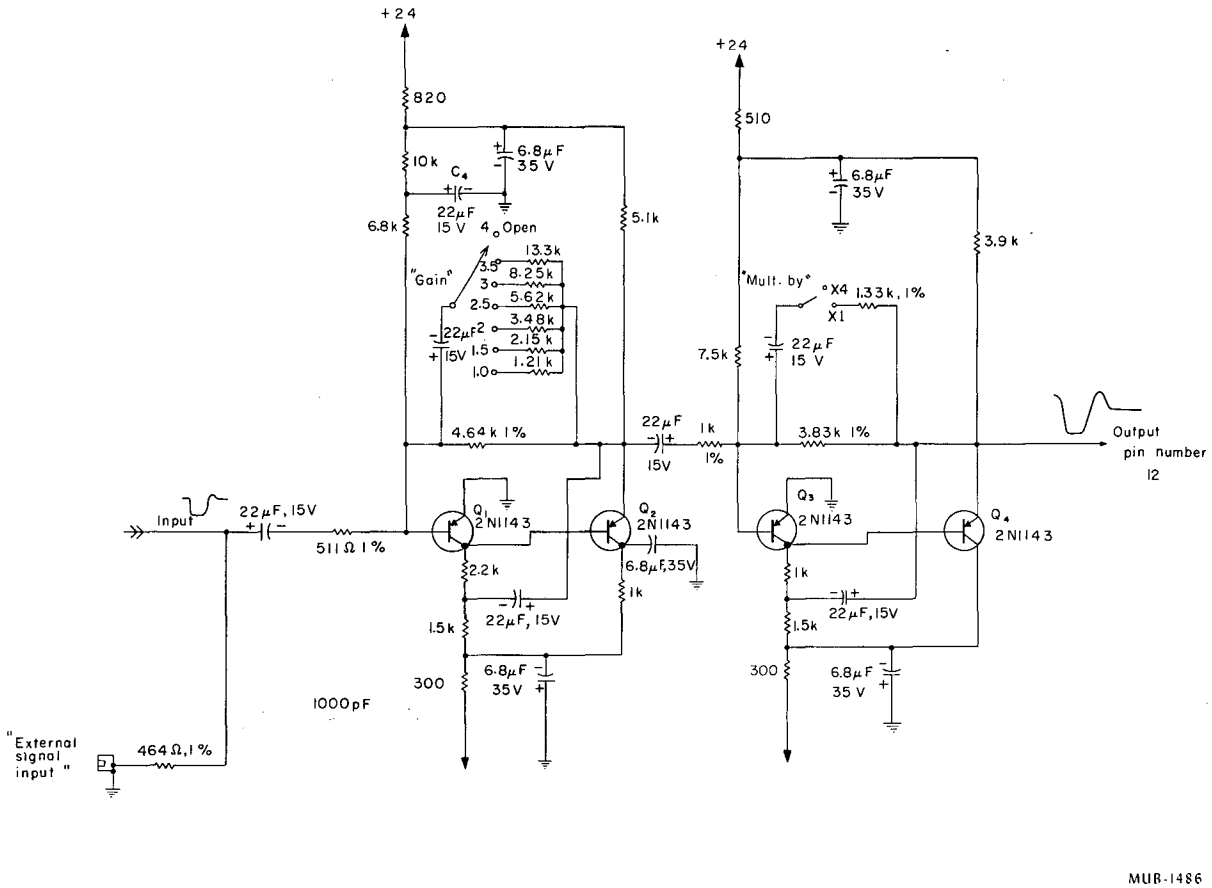

MUB-1486

Fig. 12

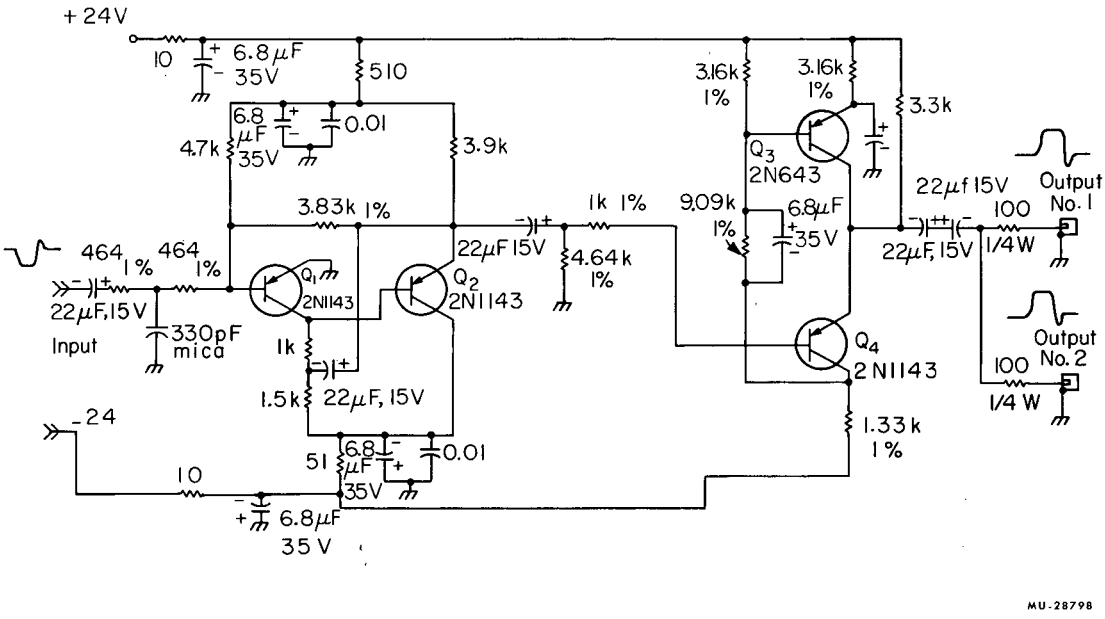
+24V
10
6.8μF 35V
510
6.8 μF 35V
0.01
4.7k
3.9k
3.83k 1%
1k 1%
9.09k 1%
6.8μF 35V
3.16k 1%
3.16k 1%
3.3k
Q3 2N643
22μf 15V
Output No. 1
100 1/4W
22μF, 15V
464 1%
464 1%
Q1 2N1143
Q2 2N1143
22μF 15V
4.64k 1%
22μF,15V
Input
330pF mica
1k
Q4 2N1143
Output No. 2
100 1/4W
1.5k
22μF, 15V
-24
51
6.8 μF 35V
0.01
1.33k 1%
10
6.8μF 35 V
MU-28798

Fig. 13

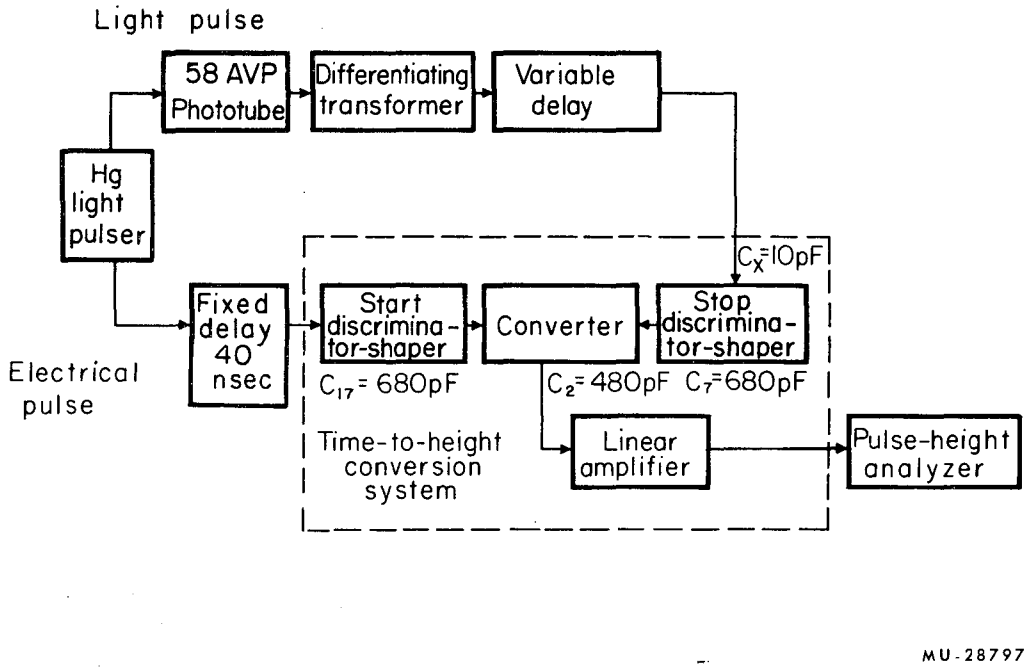
Light pulse
58 AVP Phototube
Differentiating transformer
Variable delay
Hg light pulser
C_X=10pF
Fixed delay 40 nsec
Start discrimina-tor-shaper
Converter
Stop discrimina-tor-shaper
Electrical pulse
C_{17}= 680pF
C_2= 480pF
C_7=680pF
Time-to-height conversion system
Linear amplifier
Pulse-height analyzer
MU-28797

Fig. 14